Near-Infrared Emission Spectrometry Based on an Acousto-Optical Tunable Filter

Fabiano Barbieri Gonzaga and Celio Pasquini*

Instituto de Química, Universidade Estadual de Campinas, Campinas, São Paulo, Brazil

A spectrometer has been constructed to detect the radiation emitted by thermally excited samples in the near-infrared spectral region extending from 1500 to 3000 nm. The instrument employs an acousto-optical tunable filter (AOTF) made of TeO₂ and attains maximum sensitivity by making effective use of the two diffracted beams produced by the anisotropic AOTF. The full exploitation of the transmitted power of the monochromatic beams is reported for the first time and became possible because the detector does not saturate when employed for the acquisition of the weak emission signal in the NIR region, even when exposed to the total (nondiffracted) beam. Thus, modulation and lock-in-based detection can be employed to find the intensity of the diffracted beams superimposed on the nondiffracted beam. The resolution is slighted degraded in view of the small (~10 nm) difference in the wavelength diffracted in the ordinary and extraordinary beams. The instrument has been evaluated in terms of signal-to-noise ratio, effect of sample thickness, and excitation temperature and for its potential in analytical applications in monitoring high-temperature kinetics, for qualitative identification of inorganic solids, for use with a closed cell to obtain spectra of species that evaporate at the temperatures (>150 °C) necessary for sample excitation, and for quantitative purposes in the determination of soybean oil content in olive oil. The feasibility of near-infrared emission spectroscopy has been demonstrated together with some of its advantages over mid-infrared emission spectroscopy, such as greater tolerance to sample thickness, suitable signal-to-noise, and its use in the investigation of kinetic phenomena and phase transitions at high temperatures.

Near-infrared (NIR) spectroscopy has been employed for analytical purposes based on transmittance/absorbance and reflectance measurements since the pioneering work of Norris and collaborators.[1,2] The spectral features of this region, which frequently encompass the range from 800 to 2500 nm, embody mainly overtones and combinations of fundamental vibrational energy transitions occurring in the mid-infrared region (MIR).[3,4] NIR technology has undergone a remarkable increase in its applications to real-life analytical problems and has recently been reviewed in most of its historical, fundamental, and applications aspects.[5–7] In contrast, there are few papers dealing with spectroscopic emission in the NIR region or on its exploitation for analytical purposes.[8,9]

On the other hand, the MIR has been the subject of numerous papers dealing with thermal emission of radiation.[10–28] One published work has provided a good review of the research developed in this area.[18] In these studies, a sample is thermally excited to higher vibrational energy levels and the radiant relaxation process is monitored by a spectrometer. A molecular emission spectrum is recorded whose emission maximums agree with the absorption maximums of the conventional absorbance spectra of the same samples in terms of wavelength position and relative intensities.

The evolution to high-sensitivity instruments based on Fourier transform (FT) and interferometric multiplexed spectral data acquisition is responsible for increasing interest in MIR emission

* To whom correspondence should be addressed. E-mail: pasquini@iqm.unicamp.br.

(1) Hart, J. R.; Golumbic, C.; Norris, K. H. *Cereal Chem.* **1962**, *39*, 94.
(2) Ben-Gera, I.; Norris K. H. *J. Food Sci.* **1968**, *33*, 64.
(3) Workman, J. J. *Appl. Spectrosc. Rev.* **1996**, *31*, 251−320.
(4) Williams, P.; Norris, K. *Near-Infrared Technology*, 2nd ed.; American Association of Cereal Chemistry: St. Paul, MN, 2001.
(5) Pasquini, C. *J. Braz. Chem. Soc.* **2003**, *14*, 198−219.
(6) Blanco, M.; Villarroya, I. *TrAC, Trends Anal. Chem.* **2002**, *21*, 240−250.
(7) MacClure, W. F. *J. Near Infrared Spectrosc.* **2003**, *11*, 487−518.
(8) Nelson-Avery, B. A.; Tilotta, D. C. *Appl. Spectrosc.* **1994**, *48*, 1461−1467.
(9) Ovechko, V. S.; Dmytruk, A. M.; Fursenko, O. V., Lepeshkina, T. P., *Vacuum* **2001**, *61*, 123−128.
(10) Eischens, R. P.; Pliskin, W. A. *Adv. Catal.* **1958**, *10*, 51−53.
(11) Low, M. J. D.; Inoue, H. *Anal. Chem.* **1964**, *36*, 2397−2399, 1964.
(12) Low, M. J. D.; Coleman, I. *Spectrochim. Acta* **1966**, *22*, 369−376.
(13) Griffiths, P. R. *Appl. Spectrosc.* **1972**, *26*, 73−76.
(14) Kember, D.; Chenery, D. H.; Sheppard, N.; Fell, J. *Spectrochim. Acta* **1979**, *35*, 455−459.
(15) Wagatsume, K.; Monma, K.; Suëtaka, W. *Appl. Surf. Sci.* **1981**, *7*, 281−285.
(16) Allara, D. L.; Teicher, D.; Durana, J. F. *Chem. Phys. Lett.* **1981**, *84*, 20−24.
(17) Handke, M.; Harrick, N. J. *Appl. Spectrosc.* **1986**, *40*, 401−405.
(18) Sullivan, D. H.; Conner, W. C.; Harold, M. P. *Appl. Spectrosc.* **1992**, *46*, 811−818.
(19) Keresztury, G.; Mink, J.; Kristóf, J. *Anal. Chem.* **1995**, *67*, 3782−3787.
(20) Lin, L. T.; Archibald, D. D.; Honigs, D. E. *Appl. Spectrosc.* **1988**, *42*, 477−483.
(21) Tilotta, D. C.; Busch, K. W.; Busch, M. A. *Appl. Spectrosc.* **1989**, *43*, 704−709.
(22) Pell, R. J.; Erickson, B. C.; Hannah, R. W.; Callis, J. B.; Kowalski, B. R. *Anal. Chem.* **1988**, *60*, 2824−2827.
(23) Jones, R. W.; McClelland, J. F. *Anal. Chem.* **1990**, *62*, 2074−2079.
(24) Celina, M.; Ottesen, D. K.; Gillen, K. T.; Clough, R. L. *Polym. Degrad. Stab.* **1997**, *58*, 15−31.
(25) Friedrich, M.; Zahn, D. R. T. *Appl. Spectrosc.* **1998**, *52*, 1530−1535.
(26) Kloprogge, J. T.; Frost, R. L. *Appl. Spectrosc.* **1999**, *53*, 1071−1077.
(27) Niemczyk, T. M.; Zhang, S.; Haaland, D. M. *Appl. Spectrosc.* **2001**, *55*, 1053−1059.
(28) Jones, R. W.; Meglen, R. R.; Hames, B. R.; McClelland, J. F. *Anal. Chem.* **2002**, *74*, 453−457.

spectroscopy (MIRES) because this technique lacks signal intensity, when compared with its counterpart, common absorbance spectroscopy. In fact, with few exceptions,[10,11,15] MIR emission has been investigated with the use of FT instruments.

Emission methods present some potential advantages over absorption methods. The principal is that the sample by itself is the source of the analytical information. Therefore, it can be used in probe-free methods. Also, it can be exploited in monitoring the sample directly in processes where it is already being heated or it can be heated for the purpose of emission.[22-28] A procedure based on emission frequently requires smaller amounts of samples and allows, if thermal excitation is employed, investigations of the behavior of the sample under heating. Opaque solid samples can be easily employed without any prior treatment.

The great disadvantages of the emission approach are in the low intensity of the emission signal and in the restriction of applications to thermally stable samples when quantitative or qualitative information is required although not when their thermal behavior is to be investigated. Also, for the MIR region, the low tolerance to sample thickness (only a few papers can be found where thicknesses above 100 μm have been employed[20,22,24]) has delayed the development of practical applications of the technique. Although measurable molecular emission signals can be obtained from the MIR region even by heating the sample at low temperatures (one paper reports emission from a sample at room temperature[16]), such low temperatures can produce adverse effects, which impose the need to keep the detector unit at very low temperatures[16] and to prevent against spurious emission coming from the instrument, such as the beam splitter in a FT instrument.[14]

Contrasting with the MIR region, there are few papers dealing with spectroscopic emission in the NIR region or with its exploitation for analytical purposes. In fact, a survey in the literature shows only contributions to the Astronomy and Astrophysics areas in studying the compositions of distant stars and space regions[29] and only two contributions regarding the emission of electromagnetic radiation in the NIR spectral region aiming at its use in laboratory investigation of sample composition.[8,9]

It is evident that the intensities of emission in the NIR region must decrease in a similar way as observed for absorption methods in the same spectral region when compared with the MIR region. However, in a way similar to the optical path used in absorption methods to compensate for losses in signal intensity, the temperature and sample thickness can be used to improve the signal in a NIRES method. Of course, the sample must tolerate the increase in temperature. At same time, NIRES still needs to be investigated regarding tolerances of sample thickness and the effectiveness of the emission signal to provide useful analytical information.

There is no contribution in the literature up to the moment dealing with the use of acousto-optical tunable filters (AOTF) as wavelength selectors for NIRES. The advantages of the AOTF technology and its applications in analytical spectrometry has been described and reviewed elsewhere.[30,31] Among this is the high-energy throughput, which is very attractive considering the low

signal intensities expected in NIRES. It also presents advantages regarding scan speed and robustness (nonmoving parts), provides a simple optical design for the spectrometer, and is able to scan a wide wavelength range (~1500 nm) in the NIR region (800–3000 nm), up to the border of the MIR region. The most common AOTF is based on a TeO_2 crystal driven by a $LiNbO_4$ piezoelectric transducer, which produces two monochromatic beams with close wavelengths corresponding to a given rf signal applied to the device.[31] For the purpose of absorbance measurements, one of the monochromatic beams reaches a detector and its intensity is monitored as a function of wavelength while the frequency of the rf signal (30–100 MHz, typically) is altered under control of the system computer. Use of the two diffracted beams can provide a simple design for a dual-beam instrument.[32,33] For conventional instruments employing high-power radiation sources, such as halogen filament lamps, the polychromatic radiation emitted by the source, remaining after wavelength selection by the AOTF, cannot impinge on the detector. The relative high intensity of this beam will saturate the detector, preventing signal acquisition of the much lower intensity of the monochromatic beams. This should not be the case for monitoring low-intensity signals, such as those produced by thermally excited emission in the NIR spectral region. This fact gives rise to the possibility of using the two monochromatic beams produced by anisotropic AOTFs.

This work is directed toward the development of a new NIRES instrument for measurement of near-infrared emission spectra of thermally excited samples. It employs an AOTF as wavelength selector and makes use of the full energy of the diffracted beams generated by this device. The NIRES instrument was then evaluated for its analytical potential and limitations.

Fundamentals. Molecular thermally excited emission spectroscopy has its foundations in the emission of electromagnetic radiation by heated samples. The most well known emitting system is a blackbody whose emission behavior, as a function of wavelength at absolute temperature, is described by the Planck's distribution function (H) expressed by eq 1, where λ is the

$$H(\lambda,T) = 2hc^2\{\lambda^5[\exp(hc/\lambda kT) - 1]\}^{-1} \tag{1}$$

wavelength (in meters), h, c, and k are constants, and T is the temperature (in kelvin). Equation 1 can be used to estimate the position of maximum emission for a blackbody as a function of the temperature at which it is heated. This equation is known as Wien's law and it takes the form shown in eq 2. Stephan's law

$$\lambda_{max} (\mu m) = (2.9 \times 10^3)/T \tag{2}$$

can be used to estimate the total power (E) delivered by a blackbody heated at a given temperature (eq 3).

$$E (W\ m^{-2}) = 5.69 \times 10^{-8}T^4 \tag{3}$$

A rough evaluation made with the help of eqs 2 and 3 can be employed to estimate that the minimum excitation temperature

(29) Hauser, M. G.; Dwek, E. *Annu. Rev. Astron. Astrophys.* **2001**, *39*, 249–307.
(30) Tran, C. D. *Anal. Chem.* **1992**, *64*, 971A–981A.
(31) Bei, L.; Dennis, G. I.; Miller, H. M.; Spaine, T. W.; Carnahan, J. W. *Prog. Quantum Electron.* **2004**, *28*, 67–87.

(32) Guchardi R.; Pasquini, C. *Appl. Spectrosc.* **2001**, *55*, 454–457.
(33) Kemeny, G. J.; Soryn, C. G.; Mark, H.; Rachlis, R. E.; Evans, J.; Ashraf, A. Dual Beam Acousto-Optic Tunable Spectrometer. U.S. Patent 5,039,855, 1991.

required to have a detectable NIR emission signal in the 1500–3000-nm spectral range would be ~100° C. For instance, the wavelength of maximum intensity of emission of a blackbody heated at 100 °C will be 7760 nm, well beyond the end of the NIR spectral region.

The Boltzman equation for energy distribution as a function of the temperature can also be employed to obtain an increase in the population of excited species of heated samples from the energy difference (E_j) between a given vibrational excited state and its fundamental level

$$\frac{N_j}{N_0} = \frac{P_j}{P_0} \exp\left(-\frac{E_j}{kT}\right) \qquad (4)$$

where N_j and N_0 are the number of molecules in an excited state and its fundamental level, respectively, and P_j and P_0 are statistical factors that are determined by the multiplicity of states of equal energy that may be found for each excited level of the molecule.

It is important to recall that, in the NIR spectral region, only the higher vibrationally energetic excited states, such as overtones (first, second, and third) and combinations are observed. It means that the population of potentially emitting species is low even at relatively high temperatures. Moreover, the existence of species in an excited vibrational state does not means that its relaxation to the fundamental level will occur through a radiative mechanism providing a NIR photon in the process. On the other hand, the Boltzman equation predicts an exponential increase of the excited population as a function of temperature for any excited vibrational state and, in this way, foresees a way to increase the emission signal by changing an easily controllable variable (the sample temperature).

Considering this background knowledge on the behavior of heated samples, it is possible to draw an overall picture of the emission properties in the NIR spectral region: the emission is relatively weak and higher temperatures will be required for appreciable excitation of the higher vibrational energy levels related to overtones and combinations. Conversely, the weak emission coming from the environment and instrument parts, as a result of the relatively low temperature of both the environment and the instrument in relation to the sample, should provide satisfactory measurements even in the absence of any special care regarding cooling the instrument parts or the detector.

Therefore, efforts to achieve a high signal-to-noise ratio in NIRES measurements must be focused on improvement of the energy throughput by the optics of the instrument and on energy collection by the detector.

The measured emission signal can be treated in the same way as proposed by emission in the MIR spectral region. This subject has been recently reviewed, and only the most relevant aspects will be discussed here.[19] Figure 1 shows the proposed treatment of the raw emission data in order to obtain the emissivity spectrum of a sample in the NIR region. The literature presents some controversy on the treatment of emission spectral data.[19] However, apparently there is agreement that the intensities expressed as emissivity maintain a linear relationship with the concentration of the emitting species in the sample.[19] In addition, the emissivity spectrum has been reported to better match the profile (in terms of peak format and relative intensities) of the absorption spectrum
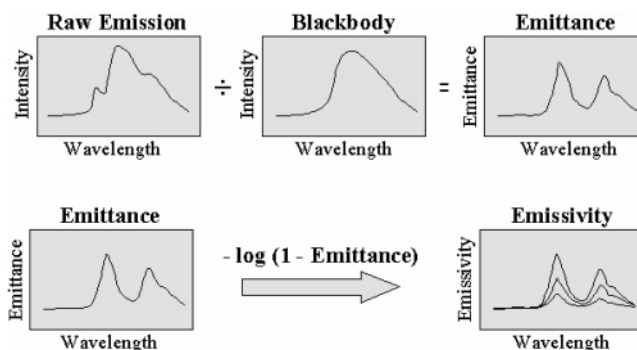
Figure 1. Data treatment of the raw emission data in order to obtain the emissivity spectrum. Three emissivity spectra are shown as the final result of data treatment in order to emphasize the linear dependence of this parameter with the concentration of the emitting species.
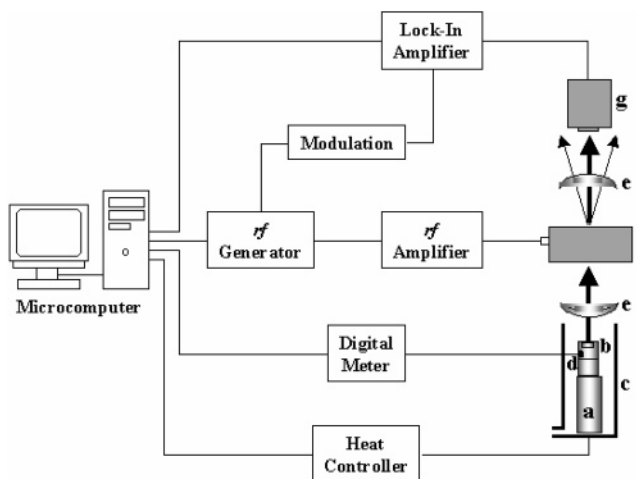
Figure 2. Schematic diagram of the proposed NIRES instrument: (a) heater; (b) emission cell; (c) acrylic jacket; (d) thermocouple; (e) CaF$_2$ lens; (f) AOTF; (g) PbS detector.

of the same material, a desirable target for emission measurements.

EXPERIMENTAL SECTION

Figure 2 shows a schematic diagram of the proposed NIRES instrument. The main features of the proposed design are in the vertical alignment of the optics, with the detector placed at 90° in relation to the plane of the output window of the AOTF, which allows for the measurement of both beams diffracted by the AOTF, superimposed on the nondiffracted beam passing straight through the device. Contrasting with absorbance measurements where a relatively high power radiation source is employed, the overall intensities for emission experiments are very low. Therefore, the full power of the nondiffracted beam leaving the AOTF can hit the detector without causing its saturation. In this way, the detector can sense the modulated fraction of the radiation whose wavelength has been selected even when superimposed on the nondiffracted and nonmodulated higher intensity beam.

The AOTF is made with a TeO$_2$ crystal, manufactured by Brimrose (TEAF_1.5–3.0) to operate in the spectral region from 1500 to 3000 nm with nominal spectral resolution varying from 9 to 37 nm as the selected wavelength increases in its useful range. The optical aperture of the device is a square window having 7-mm

sides. The AOTF was driven by a radio frequency (rf) signal generated by a digital synthesizer (Analog Devices, AD 9852), assembled to be controlled by a parallel interface (ICP-DAS A8111) placed into a microcomputer running a customized software written in Visual Basic 5.0. Under computer control, the synthesizer board generates a rf signal in the range of 68−34 MHz, necessary to select the wavelength emitted by the sample in the 1500−3000-nm range, respectively. The rf signal is modulated with a TTL level signal at 167 Hz and amplified by a rf amplifier (RF Gain, BBM2C4AJT, 8 W, 10−1000 MHz) to produce a 3.0-W signal applied to the AOTF. Therefore, the radiation of selected wavelengths is also modulated at this frequency. The modulation frequency was selected considering the results of an earlier investigation of the spectral SNR obtained by changing this parameter in the range from 150 to 500 Hz.

The more frequently employed sample cell (the open cell) was made of a rod of aluminum with an external diameter of 1.4 and 0.6 cm height, where a shallow circular groove was machined with different diameters and depths. A closed cell was also evaluated. In this case, a screw-capped cell was provided containing a glass window. The lid was attached to the end of the rod and a silicone O-ring was employed to seal the system. The cell (in its open or closed version) is attached to the top of a aluminum cylinder of the same diameter, which contains a 60-W electrical heater.

The average power applied to the heater was controlled by homemade electronic circuitry based on the duty cycle of an oscillator driven ac switch. The ratio between the on/off state of the circuit allows close control of the sample temperature at ±1 °C around the set point. The maximum temperature the present heating system can achieve is 300 °C. The entire system is contained in an acrylic tube of 3.3-cm inner diameter with 3-mm wall thickness. Nitrogen at a low flow rate can be admitted through the bottom of this tube, providing an atmosphere that is free of oxygen during sample heating. At the same time, the acrylic jacket contributes to isolate the sample from air currents, providing a more stable sample temperature. The temperature of the sample was monitored by a calibrated thermocouple inserted in a small hole drilled in the body of the cell, at the point nearest to the sample. A digital meter was set to monitor the thermocouple signal, which was connected through a RS-232 serial interface to the system-controlling computer.

The optics of the emission spectrometer consist of the already described AOTF and two CaF_2 plane-convex lenses. The arrangement was vertically positioned in relation to the sample cell in order to provide a way to work with solids as well with liquid samples using the open cell.

The detector is based on a thermoelectrically cooled (−10 °C) PbS element (Ealing Electro-Optics 043/035) and is aligned with the main nondiffracted beam coming out from the AOTF. Therefore, when no rf signal is applied to the device, a fraction of the total radiation, emitted by the sample and passing through the AOTF, reaches the detector. By applying the modulated rf signal, the light reaching the sensor becomes modulated because the two diffracted beams are alternately removed from and superimposed onto the nondiffracted beam at the modulation frequency employed. The intensity difference is the measurement of the sum of the intensities of the diffracted beams. This arrangement allows for monitoring the full power intensity of the selected wavelength of the radiation emitted by the sample. For comparison purposes, the detector has been tilted in relation to the main beam in some experiments, to monitor only one of the beams diffracted by the AOTF.

A lock-in amplifier (Stanford Research SR830 DSP) was employed for synchronous acquisition of the modulated signal (167 Hz). The analog output of the amplifier was connected to the parallel interface, which was responsible for the conversion of the analog signal to the digital domain with a 12-bit resolution.

Wavelength Calibration. The dependence of the radiation wavelength diffracted by an AOTF with the applied rf signal is not linear.[8] Therefore, a careful calibration based on standards should be provided. The present emission instrument was designed to operate at 1500−3000 nm, a spectral region that lacks standard emission lines. The region between 1500 and 2200 nm is well supplied by emissions from a low-pressure mercury lamp, and these wavelengths can be easily retrieved.[34] However, the region between 2200 and 3000 nm needs to be calibrated against the absorption bands of a silicone oil sample whose absorption spectrum was obtained with a higher resolution (4 cm^{-1}) in a FT NIR/MIR instrument (Perkin-Elmer FT-IR Spectrum GX). The same sample of silicone oil had its emissivity spectrum obtained in the proposed instrument for calibration purposes.

An exponential decay equation was generated to convert the desired wavelengths to the rf values to be applied. The set of rf values (at some predetermined nominal resolution, e.g., 5 nm) generated by the equation was stored in the computer, in binary format with a 48-bit resolution (required by the digital synthesizer), and when an emission spectrum is to be scanned, these values were successively sent to the digital synthesizer. An emission spectrum with nominal resolution of 5 nm can be scanned from 1500 to 3000 nm in 1.5 min. The calibration employed to produce the graphics of the spectra in this work was made for the two-beam arrangement.

The wavelengths selected for the ordinary and extraordinary beams leaving the AOTF were investigated by employing a low-pressure mercury lamp and looking for the four emission peaks that can be detected in the range from 1500 to 2500 nm. An average difference between the wavelength of the ordinary and extraordinary beams of 10 nm was observed in that spectral range.
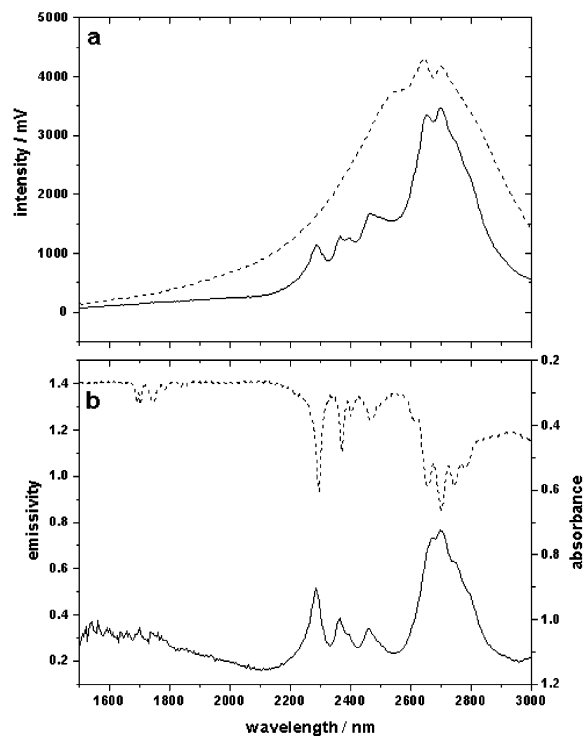
Obtaining an Emissivity Spectrum. Two cells, matched in terms of size, one containing a shallow circular groove that was blackened with matte black spray paint to approach a blackbody emitter and one whose surface has been roughly polished, were employed throughout the measurements

The emissivity spectra of solid and liquid samples were obtained by the following procedure:

1. A blackbody emission spectra is recorded at the desired temperature with an empty blackened cell that matches that for the sample.

2. A predetermined mass (3−10 mg for solids) or volume (10−50 μL for liquids) is transferred to the measurement cell, the heater is turned on, and the program waits for temperature stabilization to ±1 °C. The raw spectrum is scanned and stored in the microcomputer. Pretreatment of the solid samples can include grinding to produce a narrower range of particle size.

---

(34) http://physics.nist.gov.

Figure 3. Obtaining an emissivity spectrum. (a) Raw emission spectra of silicone oil (solid line) and blackbody (dashed line) at 220 °C. (b) Resulting emissivity spectrum (solid line) compared to absorption spectrum (dashed line).

3. Data, after subtraction of the cell emission, are processed by following the steps shown in Figure 1 to produce the emittance and emissivity spectra of the sample.

RESULTS AND DISCUSSION

The proposed spectrometer was initially evaluated by using the emission of a silicone oil sample. This compound is suitable for evaluation of the instrument performance because it is stable up to 250 °C and presents many emission/absorption bands in the region from 1600 to 3000 nm, most of which are due to the presence of Si−OH and CH_3 groups in its molecular structure.

Figure 3a shows an experimentally obtained data set necessary to produce the sample emissivity spectrum. The blackbody spectral profile reflects the performance of the detector and, to a greater extent, that of the AOTF. The loss of efficiency of the AOTF as the wavelengths move away from central values (at 2250 nm) is responsible for the overall format detected for raw emission spectra. Also it is possible to observe some humps over the blackbody profile in the range from 2600 to 2700 nm, which have been ascribed to an inherent behavior of AOTF in response to the applied rf signal.

Figure 3b compares the absorption spectrum obtained in a FT-NIR instrument with the emissivity spectrum of the same silicone oil. The absorbance and emissivity peaks shown a very good coincidence in both wavelength position and relative intensities. Differences between the spectral profiles could be attributed to the lower resolution of the AOTF-based instrument (>9 nm) when compared with the FT instrument (<1 nm). These results show that it is possible to anticipate that the emissivity spectrum carries qualitative information about the sample similar to that of the absorbance spectrum.
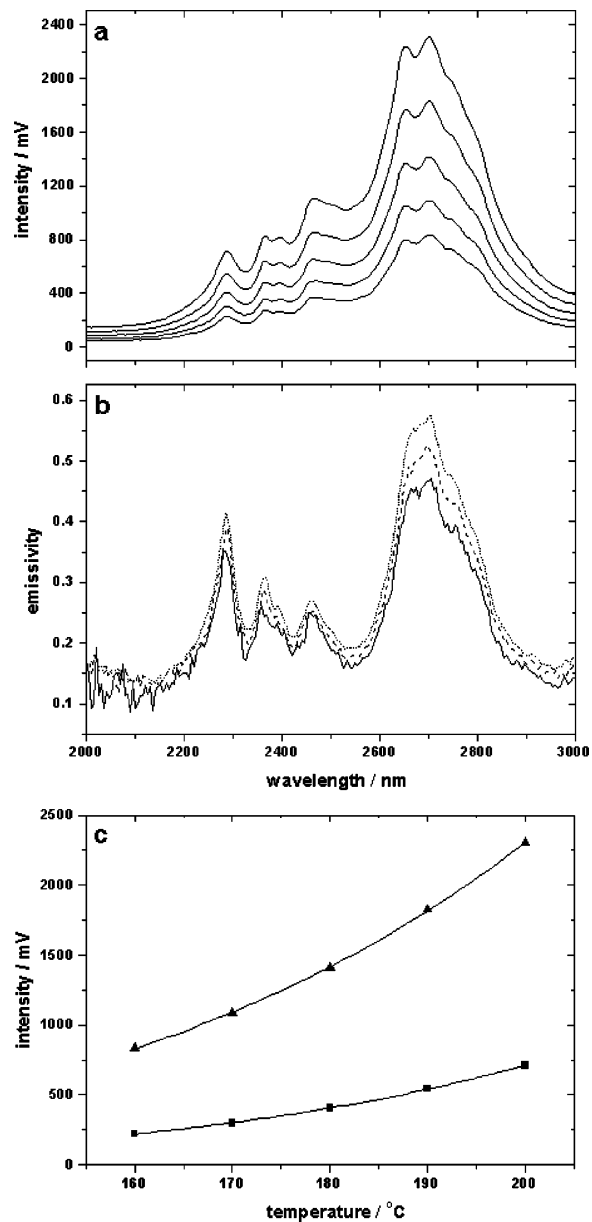
Figure 4. Effect of the sample temperature. (a) Raw emission spectra of silicone oil obtained between 160 (bottom) to 200° C (top). (b) Emissivity spectra of silicone oil at temperatures of 150 (solid line), 180 (dashed line), and 210 °C (dotted line). (c) Raw emission intensities at 2285 (square) and 2700 nm (triangle) as a function of temperature.

Effect of Sample Temperature. Figure 4 shows the effect of the sample temperature on the raw emission spectrum of the silicone oil, over the emissivity spectrum, and over the raw emission intensity for selected emission peaks. The effect is exponential for the raw emissions, as predicted by Plank's and Boltzman's laws. However, the emissivity spectra are very similar with temperature with the principal differences coming from the lower signal-to-noise ratio at lower temperatures. These data permit concluding that the emissivity spectrum supplies qualitative information about the sample that is largely independent of the temperature. However, it must be mentioned that the effectiveness of such independence is associated with the ability to obtain the blackbody reference spectrum and the sample spectrum at the same temperature.
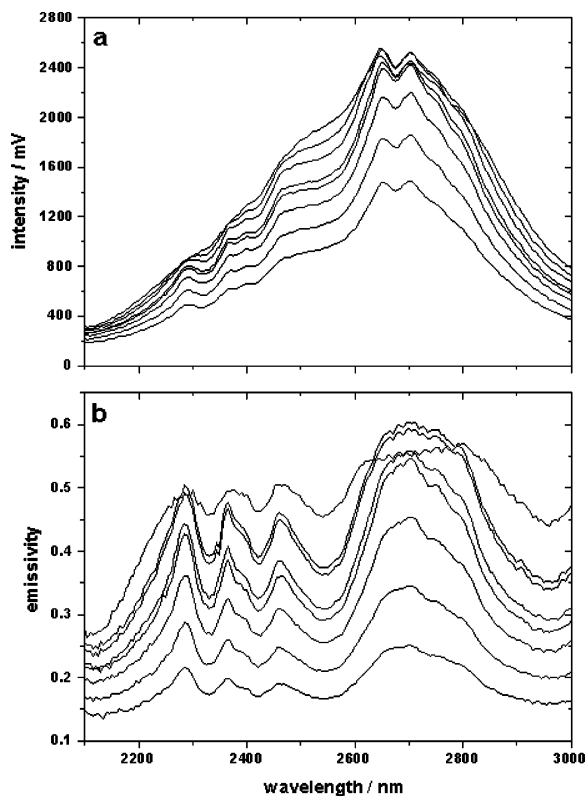
Figure 5. Effect of the sample thickness. (a) Raw emission spectra of silicone oil with thickness variation between 0.1 (bottom) to 1.5 mm (top) at 200 °C. (b) Resulting emissivity spectra.

Effect of the Sample Area and Thickness. Various sample cells were constructed with diameters of 3, 6, and 12 mm for the circular groove that contains the sample, providing samples areas of 28.3, 113.1, and 452.4 mm^2. For each diameter, a matched blackbody was produced for emittance and emissivity calculation. Sample thickness was maintained constant at 0.5 mm. The results for silicone oil show that the raw intensity increases with the sample area up to 6 mm. Larger areas produced lower intensities. The explanation for this is related to the superposition of a larger fraction of the diffracted beams on the nondiffracted beam caused by the large area of the emission source. Therefore, the modulated fraction of the emitted light sensed by the detector becomes smaller for larger area emitting sources. A sample cell diameter of 6.0 mm was selected for all further experiments.

Sample thickness has been reported as an important variable in infrared emission.[13,20,22,24] Emission spectrum in the MIR spectral region is severely affected by sample thickness due to self-absorption and temperature gradients along the sample. The overall effect represents one of the limitations of working with infrared emission in the MIR region, that is the high-absortivity coefficients which require the use of very thin samples. Typical thicknesses for MIRES experiments are in the range of a few micrometers.

Panels a and b of Figure 5 show the effect of the sample thickness over the raw emission and emissivity spectrum of silicone oil, respectively. These data were obtained by using a cell with a 6-mm-wide groove drilled with depths of 0.1−1.5 mm. The results show a high tolerance to sample thickness as far as qualitative information is concerned. It means that the emissivity data show practically the same spectral features for a wide range
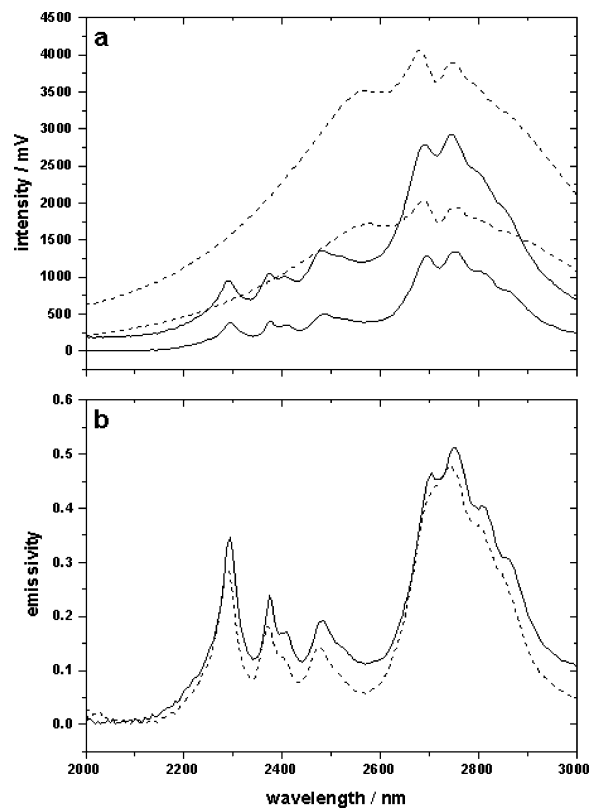
Figure 6. Comparison of the emission signals obtained by the two optical arrangements. (a) Raw emission spectra of silicone oil (solid line) and blackbody (dashed line) in two optical arrangements at 210 °C. (b) Resulting emissivity spectra from data in (a) with the detector at 90° (dashed line) and shifted 8° (solid line).

of sample thicknesses. In addition, the intensity taken at various emission peaks (at the same temperature) shows a linear behavior for thicknesses up to 0.50 mm.

These data permit concluding that there are relevant advantages of NIRES in relation to emission in the MIR region. The qualitative information is less affected by the sample thickness, larger (and easy to manage) sample thickness can be used with NIRES, and the quantitative information maintains a linear relationship with sample quantity. In addition, for the region between 1500 and 2100 nm, it is possible to obtain spectra for sample thicknesses up to 1 cm with no appreciable occurrence of self-absorption. However, in this spectral range the sensitivity is still very low.

Comparison between the Two Arrangements for Data Collection. For comparison purposes, the detector of the emission spectrometer was shifted by ∼8° in relation to the normal to the AOTF plane in order to monitor only one of the beams diffracted by the optical filter. Figure 6a shows the raw emission spectral data for a blackbody and for a silicone oil sample obtained with both arrangements. The signal intensity is doubled as expected for the frontal arrangement. In addition, the emissivity spectra obtained with both arrangements essentially show the same qualitative information, as is shown in Figure 6b for the emissivity spectra recovered from the raw emission spectra shown in Figure 6a. Because the two diffracted beams present, on average, a 10-nm difference in their wavelengths, the spectrum obtained using the sum of the two beams (observed with the 90° arrangement) shows some loss in resolution and a shift of ∼5 nm in wavelength

Table 1. Comparison of the SNR Obtained by the Two Optical Arrangements

| read type	detector position	wavelength	mean intensity	std dev	SNR
with scan	shifted 8°	2285	312.1	3.7	84
		2700	1135.2	9.6	118
	at 90°	2285	669.4	8.2	82
		2700	2363.5	16.1	147
without scan	shifted 8°	2285	322.3	3.8	85
		2700	1159.7	3.9	298
	at 90°	2285	694.9	6.7	103
		2700	2403.3	7.3	331

position of the emission peaks, when compared with that obtained for only one beam.

Signal-to-Noise Ratio Evaluation. Searching for quantitative applications of NIRES requires the evaluation of the signal-to-noise ratio (SNR) presented by the AOTF-based instrument. The results mentioned before sound promising, at least apparently, in terms of a direct improvement in the SNR achieved only by employing the arrangement at 90°, which allows for monitoring the full power of the diffracted beams. Therefore, a series of experiments were carried out in order to compare the SNR obtained by the two arrangements. First, 10 spectra from 2000 to 3000 nm, with a nominal resolution of 5 nm, were obtained at a temperature of 200 °C for a blackbody in both arrangements. The SNR for the raw emission at two different wavelengths (2250 and 2700 nm) were estimated by the standard deviation of the intensities.

Surprisingly, despite the higher signal intensity, the results show that a gain is not always achieved in the SNR when the 90° arrangement is employed (e.g., a lower SNR for 2,285 nm). A simple explanation for the observed result is in the fact that the main source for noise in the spectral data comes from the small changes in the sample temperature during the scanning (∼10 min for 10 scans). Therefore, doubling the signal is accompanied by a doubling of random intensity fluctuations due to an unsatisfactory control of sample temperature during the spectrum scan. In fact, if the rf signal is fixed at the value required to monitor only the wavelengths studied for a short time interval (5 s), during which the temperature remains essentially stable, the difference between standard deviations of the two arrangements decreases, demonstrating the real gain in the SNR for the arrangement at 90° due to the doubling of signal intensity. These data are shown in Table 1. Also, an overall inspection of data in Table 1 shows that the SNR obtained by the proposed instrument is suitable for many quantitative applications of NIRES. Furthermore, an experiment run by employing a low-pressure mercury lamp to simulate the emission source shows an effective gain close to 2 times in the signal-to-noise ratio, confirming the effectiveness of the two-beam arrangement.

A rigorous comparison of SNR values between MIRES and NIRES is presently difficult in view of the purely qualitative approach adopted for other contributions found in the literature. A visual inspection of the reported spectral results, however, permits concluding that there is a better performance of the NIRES/AOTF instrument in terms of SNR.

Qualitative Results. The proposed spectrometer has been employed in the acquisition of emissivity spectra of a number of solid and liquid samples. Figure 7 shows some results. Although,
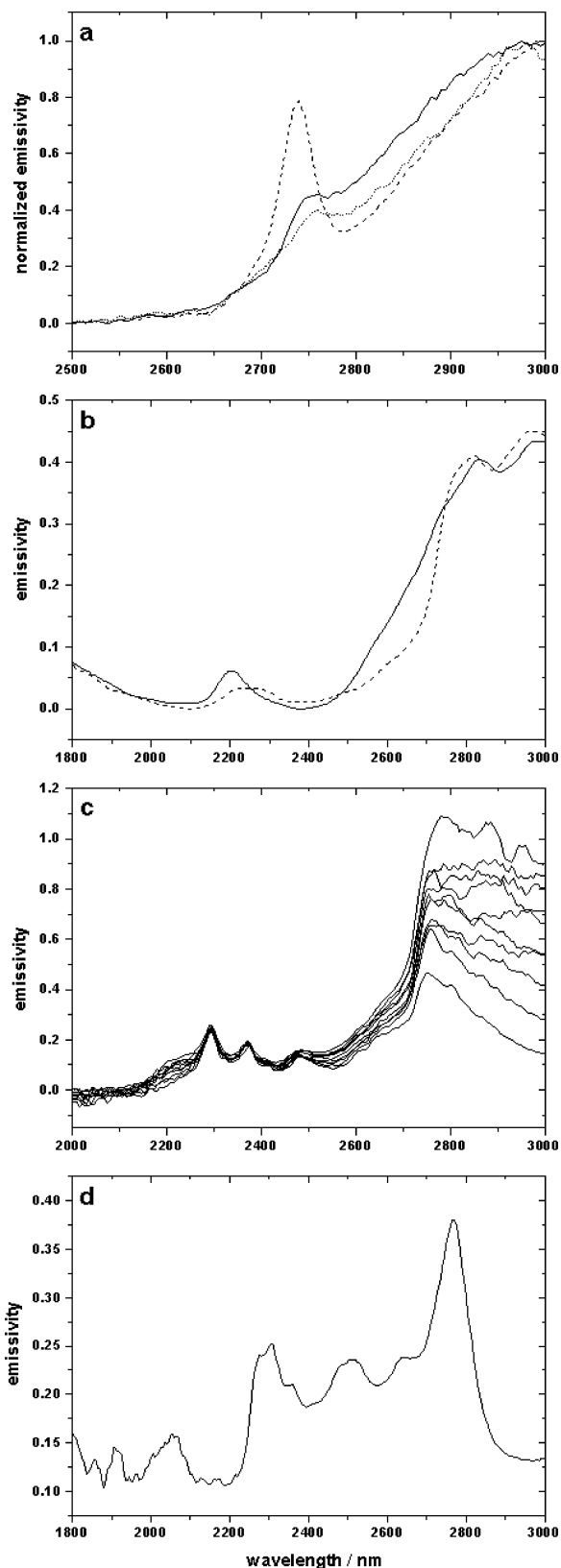
Figure 7. Some qualitative results obtained by the AOTF-based NIRES instrument. (a) Spectra, at 250 °C, of TiO_2 in rutile (solid line) and anatase forms before (dashed line) and after (dotted line) heating at 1050 °C. (b) Spectra of normal silica (solid line) and C18-modified silica (dashed line) at 250 °C. (c) Consecutive spectra (150 s apart) of silicone oil containing thermally unstable Si−H groups at 180 °C. (d) Spectrum of ethanol at 180 °C in a closed cell.

up to the moment, no interpretative insight regarding the spectral features observed in the NIR emission spectra has been attempted, it is possible to determine the qualitative potential of NIRES.

The results in Figure 7 allow predicting the use of NIRES to access the identity of solid and liquid materials without any prior treatment and reveal its potential to distinguish, for instance, between crystalline forms of the same chemical (anatase and rutile TiO_2) and surface-treated materials (silica and C18-covered silica) and for qualitative monitoring of reactions at high temperatures (silicone oil containing thermally unstable Si−H groups). In all of these examples, the quantity of the solid and liquid samples employed for the emission measurement was approximately 3 mg or 10 μL, respectively.

The emission spectrum for ethanol is also shown in Figure 7 as an example of the use of the closed cell, which allows obtaining the emission spectrum of a sample heated at temperatures above its boiling point (to 180 °C in this case). The small sample volume required for the NIRES measurement (25 μL in this case) facilitates the use of simple sealed cells with glass window.

In addition to the results shown above, raw NIRES data for lubricant oils were employed for classification of mineral- and synthetic-based products. A total of 10 μL of 12 samples of mineral and 12 samples of synthetic-based lubricants from different manufacturers were transferred to the emission cell and heated to 180 °C. The measurements were made in duplicate. The emission spectra were acquired, and the raw data in the region of 2700−2900 nm (the region that presented more spectral features) were submitted to a principal component analysis by using a chemometrics software (Unscrambler 8.0, CAMO). Spectral data were first normalized by their maximum value of emission, smoothed with a Savitsky−Golay filter employing a five-point window and second-order polynomial and then mean centered. The results for the scores in the first three principal components can be observed in Figure 8a. A clear separation between the two classes of lubricant oil is observed. There are three samples (six score values for the duplicates), which stay in the mineral class but are labeled as synthetic-based products by their manufacturer. A possible explanation is that these samples are, in fact, mixtures of mineral and synthetic brands where the mineral fraction prevails. The results achieved for lubricant oils show the potential of NIRES for qualitative applications and illustrate the fact that data conversion to emissivity may not be necessary to obtain adequate classification results obtained with chemometric multivariate data analysis.

Quantitative Results. Thirteen mixtures of edible olive and soybean oils were prepared in the laboratory to contain between 5 and 100% of authentic olive product. The mixtures were heated to 160 °C, and the emission spectra were obtained. The region between 2700 and 2900 nm of the raw emission spectra set (region that presented more spectral features) was employed for the construction of a PLS1 multivariate model utilizing two latent variables and a full cross-validation internal validation of the model aiming at the determination of soybean oil in olive oil. Spectral data were first baseline corrected, normalized by their maximum value of emission, smoothed with a three-point window moving average filter, and mean centered. The results for cross-validation are shown in Figure 8b. An absolute RMSEP of 3.2% and a correlation coefficient between the true and estimated values of
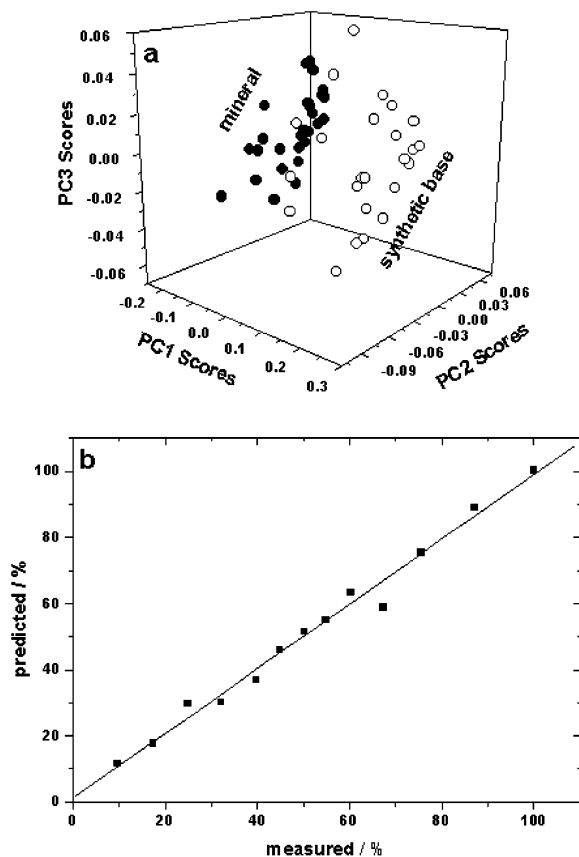
Figure 8. Results for multivariate analysis of the spectral data set for lubricant oil and quantitative results for soybean oil in olive oil. (a) Scores in the first three principal components resulting from emission spectra of mineral- and synthetic-based lubricant oils. (b) Comparison between the predicted values of soybean oil content in olive oil by PLS1 using full cross-validation with prepared values of the standards (measured).

the content of soybean oil of 0.992 were achieved. The use of the spectral data converted to emissivity prior the PLS1 modeling did not improve the final results in terms of RMSEP or correlation coefficient. This result attests to the use of NIRES in quantitative determinations employing multivariate calibration and raw emission spectrum. Although the literature recommends the use of the emissivity spectrum to overcome linearity problems, the results reported for the olive/soybean oil system indicate that multivariate calibration can overcome these sorts of problems and a good correlation between predicted and true values can be achieved over a wide concentration range.

CONCLUSION

The proposed instrument for NIRES, based on an original design employing an AOTF as wavelength selector, shows a very good performance, as shown by the results obtained for its SNR and exploratory qualitative and quantitative data. The instrument allows for increased signal intensity due to the complete detection of the two diffracted monochromatic beams generated by the AOTF. The price to pay for the gain in the SNR is lose of some spectral resolution due the small differences existing between the wavelengths of the two monochromatic beams produced by the AOTF. On the other hand, the possibility of easy interconversion between the two-beam and the one-beam arrangements (simply

by shifting the detector to a 8° geometry) allows for an increase in the dynamic range of the instrument. The one-beam arrangement is suitable for higher emitting samples or samples that can be heated to higher temperatures. At the same time, the spectrometer is simple when compared with FT instruments and can be easily assembled in many laboratories.

Evaluation of the instrument and of the potential of the NIRES technique reveals a promising field for qualitative and quantitative investigation of chemical systems at high temperature.

Temperature control of the sample has been identified as the principal variable regarding quantitative work, due the exponential dependence of emission intensity. The ±1 °C precision for sample temperature achieved with the present design of the heating device needs to be improved in order to achieve better quantitative results in the future.

On the other hand, NIRES presents some advantages that are similar to those found when absorbance in the NIR region is compared with its counterpart in the MIR spectral region. Thus, tolerance of higher sample thickness facilitates the experimental work while instrumental factors such as the possibility of using AOTF and the existence of high-performance detectors for the NIR spectral region contribute to very good quality emission measurements. In addition, sample consumption is very small with NIRES and typical masses and volumes are in the range of few milligrams or a few microliters, respectively. Opaque solids as well liquid samples can be employed directly without any prior treatment.

The outcome of an instrument is essential for analytical chemists to initiate thinking of new possibilities of application of NIRES. Based on the results reported here, it is possible to foresee interesting potential analytical applications for both NIRES and the instrumental approach described. Many industrial materials are already heated during the manufacturing processes; to mention a few: crude petroleum, polymer blends in the extruders, cements, derivatization reactions, or samples in drying and distillation processes. Some of these processes and samples are already being investigated by NIRES. In thesis, all samples heated above 100 °C would be candidates to be monitored by NIRES, with the sound advantages of working with a noninvasive technique with the sample generating the analytical information by itself.